

**Running title:** The mir-371a-373 cluster promotes the malignancy of GC

**The mir-371a-373 cluster: A crucial miRNA cluster promotes the malignancy of gastric cancer**

Zonglei Mao<sup>1,2,#,\*</sup>, Yi Pan<sup>1,2,#</sup>, Jiaping Wu<sup>1,2</sup>, Aizhai Xiang<sup>1</sup>, Kangbei Zhu<sup>1</sup>, Jiayi Li<sup>1,2</sup>, Jufeng Guo<sup>1</sup>, Ning Tang<sup>1</sup>, Jing Zhang<sup>1</sup>, Jian Liu<sup>1</sup>, Tao Rui<sup>1,2,\*</sup>

<sup>1</sup>Department of Surgery, Affiliated Hangzhou First People's Hospital, Hangzhou School of Medicine, Westlake University, Hangzhou, China; <sup>2</sup>Key Laboratory of Integrated Oncology and Intelligent Medicine of Zhejiang Province, Hangzhou, China

\*Correspondence: maoz522026820@163.com; 11818248@zju.edu.cn

#Contributed equally to this work.

**Received May 26, 2025 / Accepted September 15, 2025**

Gastric cancer is one of the most common and deadliest malignancies worldwide. Better knowledge of the risk factors for gastric cancer is essential for risk classification and therapeutic strategy evolution in gastric cancer patients. Many kinds of miRNA clusters participate in tumorigenesis and tumor progression. Herein, we sought to screen and certify the crucial miRNA cluster for prognosis prediction and potential therapeutic targets in gastric cancer. The results showed that the mir-371a-373 cluster was the most highly expressed miRNA cluster in gastric cancer. The high expression of the mir-371a-373 cluster (mir-371a, mir-372, and mir-373) was positively associated with the poor overall survival of gastric cancer patients. The expression of mir-373 was correlated with early gastric cancer recurrence. mir-373 was an independent risk factor for gastric cancer recurrence and mortality. Then, gain- and loss-of-function experiments demonstrated that mir-373 could promote the malignancy of gastric cancer cells *in vitro* and *in vivo*. Through bioinformatics analysis and experimental validation, mir-373 was correlated with tumor regulation, and ZFP91 was the direct target of mir-373. Our findings suggest that the miR-371-373 cluster, especially mir-373, could be a robust marker for the prognosis prediction of gastric cancer and a potential therapeutic target for gastric cancer.

**Key words:** gastric cancer; miRNA cluster; ZFP91; prognosis

Gastric cancer remains the fifth most commonly diagnosed cancer and the third most common cause of cancer death globally [1]. In the past two decades, therapeutic approaches, including surgery, chemotherapy, targeted therapy, radiotherapy, and even a multidisciplinary diagnosis and treatment system, have advanced [2]. However, gastric cancer patients also have a grave prognosis

[3]. In China, 80% of gastric cancer patients are confirmed to be at an advanced stage at primary diagnosis [4, 5]. Therefore, it is urgent and crucial to better explore the molecular mechanisms of gastric cancer progression and discover effective therapeutic methods.

miRNAs are characterized as a class of small noncoding RNAs with lengths of 18-25 nucleotides [6, 7]. By pairing with the 3' untranslated region of the target mRNA, miRNAs act as inhibitors by mediating repression of mRNA translation or mRNA degradation [8].

miRNAs play one of the critical roles in the regulation of tumorigenesis and tumor progression [9]. Interestingly, some miRNAs are encoded from nearby genomic regions, which are defined as miRNA clusters [10]. The transcription of miRNA clusters is characterized by a high degree of consistency [11]. The members of the miRNA cluster tend to inhibit the same target or pathways in tumors. Previous studies [12-14] confirms that some kinds of miRNA clusters present common effects on the regulation of cancer. Another study presents that CD44, KLF5, KRAS, and REAF were targeted by miR-143-145 cluster (miR-143, and miR-145) [15]. Recent research also shows that miR-29a, miR-29b, and miR-29c co-targeted GOL4A1 to inhibit the migration and invasion of gastric cancer cells [16]. Thus, the function of miRNA clusters in tumor progression is undoubtedly significant and attractive.

The mir (precursor miRNA) -371a-373 cluster is a novel cluster that contains three different pre-miRNAs (mir-373, mir-372, and mir-371a) [17]. The three members of the mir-371a-373 cluster are located on chromosome 19 (19q13.42) and are adjacent within 400 bp. The gene of mir-371a-373 cluster transcripts into pri-miR-371-3, which generates the 3 pre-miRNAs [18]. Previous studies have proven that one member of the mir-371a-373 cluster (mir-373) plays an oncogenic role in some types of cancer [19, 20]. The summary of mir-371a-373 cluster (mir-373) suggests that the role of the miR-371a-373 cluster in tumors is complex, potentially exhibiting both oncogenic and tumor-suppressive properties [21, 22]. However, to the best of our knowledge, the regulatory effect of the mir-371a-373 cluster in gastric cancer has never been systematically discussed. This study aimed to uncover that the mir-371a-373 cluster was the upregulated miRNA cluster with the highest levels in gastric cancer. The members of the mir-371a-373 cluster could also predict poor prognosis of gastric cancer. mir-373 was the key risk factor for gastric cancer recurrence and mortality. In addition, the functions and potential mechanisms of mir-373 in gastric cancer were further revealed.

74

## 75 **Patients and methods**

76 **Data acquisition and analysis.** The miRNA sequencing data, mRNA sequencing data, and matched  
77 clinical data of 411 gastric cancer samples and 42 nontumor samples were downloaded from The  
78 Cancer Genome Atlas (TCGA) database (<https://cancergenome.nih.gov/>) (Supplementary material  
79 A). By the “edgR” R software package, the differentially expressed miRNAs or mRNAs in gastric  
80 cancer samples were normalized and screened compared with nontumor samples. Log<sub>2</sub>-fold change >  
81 1 and FDR (false discovery rate) < 0.05 were set as satisfying criteria. Complete clinicopathological  
82 information of the gastric cancer patients was also obtained from the TCGA database.

83 **Cell culture.** The gastric cell lines AGS and MGC-803 were purchased from the Cell Bank of the  
84 Chinese Academy of Sciences. RPMI 1640 medium (GIBCO, USA) with 10% fetal bovine serum  
85 (BioIND, China) was used for cell culture. The cells were cultured in a humidified incubator under  
86 5% CO<sub>2</sub> at 37 °C.

87 **Plasmid construction and transfection.** To evaluate the effects of mir-373 on gastric cancer, the  
88 sequence of mir-373 or its controls were cloned and inserted into the pcDNA3.1 vector for *in vitro*  
89 experiments (Repobio, China). The transfection reagent Lipofectamine 3000 (Thermo Fisher  
90 Scientific, USA) was used to transfect the plasmid into AGS or MGC-803 cells according to the  
91 manufacturer’s instructions.

92 **Dual-luciferase reporter assay.** As described previously [14, 23], the 3’ untranslated region  
93 (3’UTR) sequences of wild-type or mutant ZFP91 were cloned and inserted into a pmirGLO vector  
94 (Repobio, China). Then, the constructed 3’UTR vectors were cotransfected with mir-373 or control  
95 plasmid into 293T cells by using Lipofectamine 3000 (Thermo Fisher Scientific, USA). After 48 h,  
96 the luciferase activity of the transfected cells was detected with a dual-luciferase reporter assay kit  
97 (Vazyme, China) according to the manufacturer’s instructions.

98 **Real-time Cell Analysis (RTCA) assay.** The cell index (CI) detected by RTCA was used to reflect  
99 cell proliferation in a label-free, real-time manner. An xCELLigence RTCA SP instrument equipped  
100 with E-Plate 96 was used for cell proliferation. The pretreated cells were seeded in an E-Plate 96.  
101 According to the manufacturer’s instructions, the CI was detected for 72 h with an interval of 1 h.

102 **Cell counting kit-8 (CCK-8) assay.** Cell proliferation was detected by the CCK-8 assay. The  
103 pretreated cells in 96-well plates were incubated with CCK-8 reagent (Dojindo Molecular

Technologies, Japan) for 0.5 h or 1 h. The absorbance at 450 nm was detected using a spectrophotometric reader (Multiskan FC, Thermo Scientific) to reflect the proliferation efficiency.

**Transwell assay.** The Transwell system (Corning Inc.) was used for the cell migration and invasion assay. For the invasion assay, the upper chamber of the Corning Transwell membrane was precoated with Matrigel (BD Biosciences, USA). In the migration assay, the Matrigel was free. The pretreated cells were resuspended in the Transwell system and cultivated for 24 h. The chambers were fixed with 4% paraformaldehyde fix solution and stained with crystal violet. The number of stained cells was used to reflect invasion and migration ability.

**Quantitative Reverse Transcription PCR (qRT-PCR).** As previously detailed, total RNA was extracted and purified from tissue samples using the RNA-Quick Purification Kit (RN001, esunbio, China) following the manufacturer's instructions. For the reverse transcription of small RNAs, stem-loop reverse transcription primers were employed according to the protocol of the riboSCRIPT Reverse Transcription Kit (#C11027, Ribobio, China). PCR amplification utilized the 2× Universal SYBR Green Fast qPCR Mix (#RK20433, Abclonal, China) with cycling conditions of 95 °C for 15 seconds and 60 °C for 30 s. U6 snRNA (Bulge-Loop U6 qPCR Primer (#MQPS0000002, Ribobio, China) served as the normalization control for small RNAs. The sequences of all primers used in this study are provided in Supplementary Table S1.

**Western blot analysis.** As described previously [23], all the quantified and boiled proteins were electrophoresed on a 10% SDS-PAGE gel (#FD341-100, Fudebio, China) and then transferred onto equilibrated polyvinylidene difluoride (PVDF) membranes. The membranes were blocked for 1 h at room temperature and incubated with anti-ZFP91 antibody (Absin, #abs101676, China) or anti-AKIP1 (#PA5-106533, Thermo Fisher, USA) overnight at 4 °C. After the membranes were incubated with secondary anti-rabbit immunoglobulin G horseradish peroxidase (HRP)-linked antibody (ABclonal, #AS014, China), the bands were detected by an enhanced chemiluminescence (ECL) system (Biotanon, China) with FDbio-FemtoECL (#FD8380, Fudebio, China).

**Potential target prediction and miRNA pathway analysis.** The professional online miRNA targets analysis database TargetScan ([https://www.targetscan.org/vert\\_80/](https://www.targetscan.org/vert_80/)) was used to screen the potential targets of miRNAs [24, 25]. To analyze the bioinformatic function of miRNAs, Kyoto Encyclopedia of Genes and Genomes (KEGG) and Gene Ontology analyses were performed to investigate the functional pathways of the target genes by the online database “KOBAS 3.0”

134 (kobas.cbi.pku.edu.cn).

135 **Tumor model.** The tumor model was performed as described previously [23]. Balb/c male nude  
136 mice (6 weeks old) were obtained from the Shanghai Experimental Animal Center, Chinese  
137 Academy of Science. All methods were conducted according to the criteria of the National Institute  
138 Guide for the Care and Use of Laboratory Animals and with the ARRIVE guidelines. The animal  
139 research protocol was approved by the Institutional Animal Care and Use Committee (IACUC),  
140 Zhejiang Center of Laboratory Animals (ZJCLA, Approval No. ZJCLA-IACUC-20010185). Before  
141 the mice were injected with the stably expressing mir-373 and mir-ctrl AGS cells, they were  
142 randomly assigned to each group. Then, the cells were subcutaneously injected into the right flank  
143 of the mice (n=5 in each group). Beginning on day 7, all the tumor sizes of the mice were measured  
144 every 3 days. On day 26, the mice were anesthetized and euthanized with CO<sub>2</sub> inhalation before  
145 being sacrificed.

146 **Statistical analysis.** The quantitative variables are described as the mean±standard deviation (SD)  
147 or median±interquartile range (IQR). Student's t test, Mann-Whitney test, or one-way analysis of  
148 variance (ANOVA) followed by a post hoc Bonferroni's test were performed for the comparison of  
149 the quantitative variables. The chi-square test or Fisher's exact test was performed for the  
150 comparison of categorical measures. The linear associations between two sets of data were assessed  
151 by using the Pearson correlation coefficient. Kaplan-Meier survival curves were analyzed with the  
152 log-rank test. Univariate and multivariate Cox proportional hazards regression models were used to  
153 evaluate the risk factors for gastric cancer. The optimal cutoff values of mir-371a, mir-372, and  
154 mir-373 for predicting the prognosis of gastric cancer were detected with the receiver operating  
155 characteristic (ROC) curve and calculated with the best Youden index. The results of the *in vitro*  
156 experiments were obtained from three independent experiments. Statistical analysis was performed  
157 with SPSS Software (Version 19.0), and a p-value < 0.05 was set as the significance level. P-values  
158 \* < 0.05, \*\* < 0.01, \*\*\* < 0.001, and \*\*\*\* < 0.0001 and, respectively.

159

## 160 **Results**

161 **Robustly high expression level of the mir-371a-373 cluster in gastric cancer.** We acquired the  
162 total miRNA profiles of 411 gastric cancer samples and 42 nontumor samples from the TCGA  
163 database. As previously described, with the analysis of the “edgeR” package, the differentially

expressed pre-miRNAs in gastric cancer are shown as the log<sub>2</sub>-fold-change values compared with those in the nontumor samples (Supplementary material B). We found that the mir-371a-373 cluster (mir-373, mir-372, and mir-371a) was dramatically upregulated in gastric cancer. Among all overexpressed pre-miRNAs, mir-373 and mir-372 ranked 3rd and 4th respectively, and another member of the mir-371a-373 cluster (mir-371a) ranked 16th (Figure 1A). mir-373, mir-372 and mir-371a rose by 6.87, 7.07 and 6.19 (log<sub>2</sub>-change) in gastric cancer, respectively. Then, we extracted and visualized all the data in scatter plots and unsupervised hierarchical clustering. All three members of the mir-371a-373 cluster were significantly upregulated in gastric cancer samples compared with nontumor tissues (Figures 1B, 1C). Furthermore, we evaluated the expression levels of the mir-371a-373 cluster in 25 paired gastric cancer tissues and their adjacent non-tumorous counterparts from our cohort. The analysis revealed that mir-373, mir-372, and mir-371a were all upregulated in gastric cancer samples. Notably, mir-373 exhibited the most significant differential expression, with high expression observed in 22 out of the 25 pairs.

**High expression of the mir-371a-373 cluster predicted the unfavorable prognosis of gastric cancer.** Upregulation of the mir-371a-373 cluster indicated that they might have significant effects on the tumor progression of gastric cancer. By collecting the clinical information of gastric cancer patients, we evaluated the correlation between the expression levels of the mir-371a-373 cluster and gastric cancer recurrence and mortality. Kaplan-Meier analysis with the log-rank test confirmed that the high expression of all three members of the mir-371a-373 cluster (mir-373, mir-372, and mir-371a) was positively associated with poor survival in gastric cancer (Figure 2A). The gastric cancer patients who expressed higher levels of mir-373, mir-372, and mir-371a had a worse 3-year cumulative survival rate (Figure 2B) and median survival time (Figure 2C). Among them, the patients with high expression of mir-373 had a 3-year cumulative survival rate of only 13.1% and a median survival time of only 300 days. Among the three members of the miR-371a-373 cluster, only miR-373 could predict the early tumor recurrence of gastric cancer (Figure 2D). The patients with high expression of mir-373 presented a poor 3-year disease-free survival rate of only 27.9% (Figure 2E) and a median disease-free survival time of only 487 days (Figure 2F). The mir-371a-373 cluster, especially mir-373, demonstrated significant predictive value for gastric cancer early recurrence and mortality.

**mir-373 was a significant and independent risk factor for gastric cancer recurrence and**

194 **mortality.** Considering that the mir-371a-373 cluster could predict the poor prognosis of gastric  
195 cancer, we further evaluated the role of the mir-371a-373 cluster in the risk factor evaluation of  
196 gastric cancer. By univariate Cox analysis, we showed that all the members of the mir-371a-371  
197 cluster, tumor location, tumor stage, age, T stage, N stage and M stage were risk factors for overall  
198 survival in gastric cancer (Figure 3A). Then, we enrolled all the elements in the multivariate Cox  
199 model. The results showed that mir-373, mir-371a, M-stage, and T-stage were independent risk  
200 factors for gastric cancer mortality (Figure 3B). mir-373 was the most critical risk factor with the  
201 highest HR value (HR: 2.278, 95% CI: 1.236-4.198, p=0.008). When we evaluated the risk factors  
202 for gastric cancer early recurrence by univariate Cox analysis, we found that mir-373, tumor  
203 location, and N-stage, but not mir-371a and mir-372, were risk factors for gastric cancer early  
204 recurrence (Figure 3C). Then, by multivariate Cox analysis, mir-373 was confirmed as an essential  
205 independent risk factor for gastric cancer early recurrence (HR: 2.399, 95% CI: 1.139-5.051,  
206 p=0.021, Figure 3D). The results proved that mir-373 must be a crucial factor in gastric cancer early  
207 recurrence and mortality. Then, we assessed the correlation between mir-373 and the  
208 histopathologic characteristics. We found that mir-373 was associated with tumor recurrence  
209 (p=0.036), tumor events (p=0.007), and tumor status (p=0.021) (Supplementary Table S2). All the  
210 results suggested that among the three members of the mir-371a-373 cluster, mir-373 was a  
211 significant and independent risk factor for gastric cancer recurrence and mortality.

212 **mir-373 promoted the proliferation, invasion, and migration of gastric cancer *in vitro* and *in***  
213 ***vivo*.** Given that mir-373 showed the most pronounced differential expression within the  
214 mir-371a-373 cluster and was associated with gastric cancer prognosis, we further investigated the  
215 effects of mir-373 on the tumor progression of gastric cancer cells. The CCK-8 assay confirmed that  
216 mir-373 overexpression promoted the proliferation of AGS and MGC-803 cells compared with the  
217 controls (Figure 4A, Supplementary Figure S2A). Then, the functions of mir-373 were competitively  
218 inhibited by the transfection of mir-373 inhibitor. The CCK-8 assay also proved that the mir-373  
219 inhibitor decreased the growth of AGS cells (Figure 4A). RTCA showed that  
220 mir-373-overexpressing AGS cells presented a faster real-time growth curve, while  
221 mir-373-inhibited AGS cells showed the opposite results (Figure 4B). The transwell assay was used  
222 to assess the invasion and migration of mir-373 in gastric cancer (Figures 4C, 4D; Supplementary  
223 Figures S2B, S2C). The results proved that mir-373 overexpression could significantly enhance the

224 invasion and migration of AGS and MGC-803 cells. The invasion capacity could also be inhibited  
225 by mir-373 inhibition (Figures 4C, 4D). The AGS cells stably expressing mir-373 and mir-ctrl were  
226 used to established the nude gastric cancer model. The results showed that mir-373 promoted the  
227 growth of gastric cancer *in vivo*, after the tumor volume was measured (Figure 4E).

228 **mir-373 promoted the malignancy of gastric cancer by directly targeting ZFP91.** We confirmed  
229 that mir-373 was a significant risk factor for gastric cancer. Thus, we hypothesized that the potential  
230 mechanisms of mir-373 in gastric cancer might be related to cancer regulation pathways. The genes  
231 that were significantly correlated with the expression of mir-373 were enrolled in Gene Ontology  
232 and KEGG analyses. Several cancer-related pathways were enriched, including pathways in cancer  
233 and microRNAs in cancer (Figure 5A). Their biological function focused on transcription regulation  
234 (Figure 5B).

235 In general, miRNAs work on biological processes by suppressing the transcription or transcript  
236 translation of target genes [26]. To investigate the potential targets of mir-373, 3 conditions were set  
237 in this study: i) downregulated genes of gastric cancer from the TCGA database, ii) significantly  
238 and negatively correlated with the expression of mir-373, and iii) potential target genes of mir-373  
239 from the TargetScan database that showed potential target sites. Thus, from the TCGA database, 22  
240 genes were downregulated and negatively correlated with mir-373 in gastric cancer. After  
241 overlapping with the TargetScan database, ZFP91 and AKIP1 were screened as potential targets of  
242 mir-373 in gastric cancer, which were enrolled in the experimental validation (Figure 5C).

243 AGS and MGC-803 cells were transfected with mir-373 overexpression vector and its control  
244 (miR-ctrl). The results showed that ZFP91, but not AKIP1, was inhibited by mir-373 (Figure 5D).  
245 The 3' UTR sites of ZFP91 (wild-type) and its mutant counterparts were cloned and inserted into  
246 luciferase reporter vectors. The luciferase reporter assay showed that mir-373 significantly inhibited  
247 the luciferase activity of the wild-type vector (Figures 5E, 5F). Thus, we confirmed that ZFP91 was  
248 the direct target of mir-373 in gastric cancer.

249 We also showed that ZFP91 was a negative mediator of the malignancy of gastric cancer. The  
250 log-rank test showed that gastric cancer with lower expression of ZFP91 was associated with poorer  
251 survival ( $p=0.035$ ) (Supplementary Figure S3A). The median survival (MS) of gastric cancer  
252 patients with low ZFP91 was 782 days (95% CI: 588-975). However, that with high ZFP91 was  
253 1686 days (95% CI: 603-2768). Multivariate Cox analysis showed that ZFP91 was a protective



254 factor against the mortality of HCC (Supplementary Figure S3B). When analyzing the correlation  
255 between ZFP91 and the clinicopathological characteristics, we found that ZFP91 was negatively  
256 associated with T4 status (invasion of plasma membranes or adjacent tissues or organs)  
257 (Supplementary Table S3). This result indicated that gastric cancer with low ZFP91 had much more  
258 invasive and aggressive phenomena.

259 Rescue experiments were performed to prove that mir-373 promoted the malignancy of gastric  
260 cancer by directly targeting ZFP91. When cotransfected with mir-373 and ZFP91, the proliferation  
261 and invasion of gastric cancer, which were inhibited by mir-373, could be significantly rescued by  
262 the overexpression of ZFP91 (Figures. 5G-5I, Supplementary Figure S4).

263

## 264 Discussion

265 It is crucial to better understand gastric cancer tumorigenesis and to discover effective therapeutic  
266 targets for gastric cancer. In recent decades, there has been a great advance in the research of  
267 cancer-related miRNA clusters. First, miRNA clusters were considered to be rare and notable  
268 members of the miRNA family. In contrast, after exploring the miRbase database, we found that  
269 nearly half of the miRNAs (more than 400) originated from miRNA clusters. This result suggested  
270 that the origin of the miRNA cluster was not accidental and was related to species evolution. A  
271 professional review proposed a diversity of modes of the evolutionary provenance of miRNA  
272 clusters, including local duplication, de novo hairpin birth, tandem duplication, cluster fission, and  
273 new miRNA acquisition [27]. Another review also proposed a "functional coadaptation" model to  
274 explain that the clustering of miRNA assisted in miRNAs survival and development of functions  
275 [28].

276 A large number of reports thus far have proven that disorders of miRNA clusters could lead to  
277 tumorigenesis and tumor progression. Our previous study showed that C19MC plays an essential  
278 role in the increase in the HCC tumor burden [13]. The members of C19MC, miR-516a-3p,  
279 miR-512-3p, and miR-519a-5p, can significantly promote the malignancy of HCC *in vivo* and *in*  
280 *vitro* [14, 23]. We also demonstrated that the miR-767-105 cluster is crucial for predicting the poor  
281 prognosis of hepatocellular carcinoma [12]. A prior study described the fundamental mechanisms of  
282 regulation and reviewed the biological functions of numerous miRNA clusters in detail [11].  
283 However, as a whole, the effects of the mir-371a-373 cluster on tumors have rarely been reported. A

284 recent study proved that deletion of the mir-371a-373 cluster by the CRISPR-Cas9 system could  
285 decrease the oncogenic capacity of oral squamous cell carcinoma, while activation of the  
286 mir-371a-373 cluster had the opposite effects [29]. Our study discovered that the mir-371a-373  
287 cluster was the most significantly upregulated cluster in gastric cancer. All three members of the  
288 mir-371a-373 cluster predicted the poor overall survival of gastric cancer, and only mir-373  
289 predicted the poor disease-free survival of gastric cancer. By multivariate Cox analysis, mir-373  
290 was confirmed to be a significant and independent risk factor for gastric cancer recurrence and  
291 mortality. Meanwhile, mir-373 was the factor associated with high risk. Thus, the results showed  
292 that mir-373 could be an ideal biomarker for the prediction of gastric cancer prognosis.

293 The functions of mir-373 in many kinds of cancers have been clarified. For example, mir-373  
294 promoted the metastasis of tongue squamous cell carcinoma by targeting WNT signaling pathway  
295 inhibitor 1 (DKK1) [30]. Existing evidence presented that mir-373 stimulated cell migration and  
296 invasion of breast cancer cells and was further associated with the cancer migration phenotype [31].  
297 Furthermore, another research summarized that mir-373 promoted cancer cell proliferation,  
298 apoptosis, mesendoderm differentiation and migration. However, it also yields the opposite effects  
299 [22]. In this study, we confirmed that mir-373 significantly boosted the proliferation, migration, and  
300 invasion of gastric cancer. The results further validated that mir-373 was the key factor for the  
301 regulation of gastric cancer.

302 We uncovered that ZFP91 was the direct target of mir-373 in gastric cancer. ZFP91 is a member of  
303 the zinc finger protein family and serves as an E3 ubiquitin ligase that ubiquitinates proteins such as  
304 NF- $\kappa$ B-inducing kinase (NIK), forkhead Box A1 (FOXA1), and heterogeneous nuclear  
305 ribonucleoprotein (hnRNP) [32-34]. It contains 5 zinc finger domains and some nuclear localization  
306 signals. However, its roles in tumorigenesis among many types of cancers are indeterminate. ZFP91  
307 promotes tumor progression in acute myelogenous leukemia, prostate cancer, and colon cancer  
308 [35-37]. ZFP91 can also act as a tumor suppressor gene. In hepatocellular carcinoma (HCC), ZFP91  
309 suppresses HCC glucose metabolism reprogramming, cell proliferation and metastasis by inhibiting  
310 hnRNP A1-dependent pyruvate kinase M (PKM) splicing [34]. Previous research reported that  
311 ZFP91 causes E2F2 polyubiquitination and leads to the transcriptional suppression of oncogenes in  
312 an HCC cell line [38]. Moreover, another team suggested that lnc-CTSLP4 inhibits  
313 epithelial-mesenchymal transition (EMT) and metastasis of gastric cancer by recruiting ZFP91 to

314 induce the degradation of heterogeneous nuclear ribonucleoprotein AB (HNRNPAB) [39]. Our  
315 results suggested that mir-373 could promote the tumorigenesis of gastric cancer by directly  
316 inhibiting the expression of ZFP91. We found that ZFP91 was a negative mediator in gastric cancer,  
317 which is in agreement with the results from Pan T et al [39].

318 In general, our study identified a particular miRNA cluster in gastric cancer. The miR-371-373  
319 cluster, especially mir-373, was proven to be useful for predicting the prognosis of gastric cancer.  
320 Meanwhile, the miR-371-373 cluster could be a potential therapeutic target for gastric cancer.  
321 mir-373 promoted the malignancy of gastric cancer by directly targeting ZFP91. As future  
322 perspectives, we attempted to explore the application of the miR-371-373 cluster as a biomarker in  
323 serum liquid biopsy by acquiring a minimum amount of serum for early gastric cancer diagnosis  
324 and prognosis prediction.

325

326 Acknowledgements: This study was supported by the Zhejiang Provincial Natural Science  
327 Foundation of China (LQ23H160045), the Hangzhou Joint Fund of the Zhejiang Provincial Natural  
328 Science Foundation of China (LHZY24H300003) and Medical Health Science and Technology  
329 Project of Zhejiang Provincial Health Commission, China (2023RC224, 2023RC220, 2024KY189,  
330 and 2024KY1321).

331

332 **Supplementary data are available in the online version of the paper.**

333

334

## 335 **References**

- 336 [1] SMYTH EC, NILSSON M, GRABSCH HI, VAN GRIEKEN NC, LORDICK F. Gastric  
337 cancer. *Lancet* 2020; 396: 635-648. [https://doi.org/10.1016/S0140-6736\(20\)31288-5](https://doi.org/10.1016/S0140-6736(20)31288-5)
- 338 [2] VENERITO M, VASAPOLLI R, ROKKAS T, MALFERTHEINER P. Gastric cancer:  
339 epidemiology, prevention, and therapy. *Helicobacter* 2018; 1: e12518.  
340 <https://doi.org/10.1111/hel.12518>
- 341 [3] CHEN GM, YUAN SQ, NIE RC, LUO TQ, JIANG KM et al. Surgical Outcome and  
342 Long-Term Survival of Conversion Surgery for Advanced Gastric Cancer. *Ann Surg Oncol*  
343 2020; 27: 4250-4260. <https://doi.org/10.1245/s10434-020-08559-7>
- 344 [4] GAO K, WU J. National trend of gastric cancer mortality in China (2003-2015): a  
345 population-based study. *Cancer Commun (Lond)* 2019; 39: 24.  
346 <https://doi.org/10.1186/s40880-019-0372-x>

- 347 [5] Strong VE, Wu AW, Selby LV, Gonen M, Hsu M et al. Differences in gastric cancer survival  
348 between the U.S. and China. *J Surg Oncol* 2015; 112: 31-37.  
349 <https://doi.org/10.1002/jso.23940>
- 350 [6] LEE RC, FEINBAUM RL, AMBROS V. The *C. elegans* heterochronic gene *lin-4* encodes  
351 small RNAs with antisense complementarity to *lin-14*. *Cell* 1993; 75: 843-854.  
352 [https://doi.org/10.1016/0092-8674\(93\)90529-y](https://doi.org/10.1016/0092-8674(93)90529-y)
- 353 [7] FILIPOWICZ W, BHATTACHARYYA SN, SONENBERG N. Mechanisms of  
354 post-transcriptional regulation by microRNAs: are the answers in sight. *Nat Rev Genet*  
355 2008; 9: 102-114. <https://doi.org/10.1038/nrg2290>
- 356 [8] DALMAY T. Mechanism of miRNA-mediated repression of mRNA translation. *Essays*  
357 *Biochem* 2013; 54: 29-38. <https://doi.org/10.1042/bse0540029>
- 358 [9] BERINDAN-NEAGOE I, MONROIG PDEL C, PASCULLI B, CALIN GA.  
359 MicroRNAome genome: a treasure for cancer diagnosis and therapy. *CA Cancer J Clin*  
360 2014; 64: 311-336. <https://doi.org/10.3322/caac.21244>
- 361 [10] ALTUVIA Y, LANDGRAF P, LITHWICK G, ELEFANT N, PFEFFER S et al. Clustering  
362 and conservation patterns of human microRNAs. *Nucleic Acids Res* 2005; 33: 2697-2706.  
363 <https://doi.org/10.1093/nar/gki567>
- 364 [11] KABEKKODU SP, SHUKLA V, VARGHESE VK, D' SOUZA J, CHAKRABARTY S et al.  
365 Clustered miRNAs and their role in biological functions and diseases. *Biol Rev Camb Philos*  
366 *Soc* 2018; 93: 1955-1986. <https://doi.org/10.1111/brv.12428>
- 367 [12] RUI T, XU S, FENG S, ZHANG X, HUANG H et al. The mir-767-105 cluster: a crucial  
368 factor related to the poor prognosis of hepatocellular carcinoma. *Biomark Res* 2020; 8: 7.  
369 <https://doi.org/10.1186/s40364-020-0186-7>
- 370 [13] RUI T, XU S, ZHANG X, HUANG H, FENG S et al. The chromosome 19 microRNA  
371 cluster, regulated by promoter hypomethylation, is associated with tumour burden and poor  
372 prognosis in patients with hepatocellular carcinoma. *J Cell Physiol* 2020; 235: 6103-6112.  
373 <https://doi.org/10.1002/jcp.29538>
- 374 [14] RUI T, ZHANG X, FENG S, HUANG H, ZHAN S et al. The Similar Effects of miR-512-3p  
375 and miR-519a-2-5p on the Promotion of Hepatocellular Carcinoma: Different Tunes Sung  
376 With Equal Skill. *Front Oncol* 2020; 10: 1244. <https://doi.org/10.3389/fonc.2020.01244>
- 377 [15] PAGLIUCA A, VALVO C, FABRIZI E, DI MARTINO S, BIFFONI M et al. Analysis of the  
378 combined action of miR-143 and miR-145 on oncogenic pathways in colorectal cancer cells  
379 reveals a coordinate program of gene repression. *Oncogene* 2013; 32: 4806-4813.  
380 <https://doi.org/10.1038/onc.2012.495>
- 381 [16] CHENG J, ZHUO H, WANG L, ZHENG W, CHEN X et al. Identification of the  
382 Combinatorial Effect of miRNA Family Regulatory Network in Different Growth Patterns of  
383 GC. *Mol Ther Oncolytics* 2020; 17: 531-546. <https://doi.org/10.1016/j.omto.2020.03.012>
- 384 [17] KOZOMARA A, BIRGAOANU M, GRIFFITHS-JONES S. miRBase: from microRNA  
385 sequences to function. *Nucleic Acids Res* 2019; 47: D155-D162.  
386 <https://doi.org/10.1093/nar/gky1141>
- 387 [18] VOORHOEVE PM, LE SAGE C, SCHRIER M, GILLIS AJ, STOOP H et al. A genetic  
388 screen implicates miRNA-372 and miRNA-373 as oncogenes in testicular germ cell tumors.  
389 *Cell* 2006; 124: 1169-1181. <https://doi.org/10.1016/j.cell.2006.02.037>

- 390 [19] LI LY, WANG XL, WANG GS, ZHAO HY. MiR-373 promotes the osteogenic  
391 differentiation of BMSCs from the estrogen deficiency induced osteoporosis. *Eur Rev Med*  
392 *Pharmacol Sci* 2019; 23: 7247-7255. [https://doi.org/10.26355/eurrev\\_201909\\_18827](https://doi.org/10.26355/eurrev_201909_18827)
- 393 [20] FAN X, XU S, YANG C. miR-373-3p promotes lung adenocarcinoma cell proliferation via  
394 APP. *Oncol Lett* 2018; 15: 1046-1050. <https://doi.org/10.3892/ol.2017.7372>
- 395 [21] SHAH JA, KHATTAK S, RAUF MA, CAI Y, JIN J. Potential Biomarkers of miR-371-373  
396 Gene Cluster in Tumorigenesis. *Life (Basel)* 2021; 11: 984.  
397 <https://doi.org/10.3390/life11090984>
- 398 [22] WEI F, CAO C, XU X, WANG J. Diverse functions of miR-373 in cancer. *J Transl Med*  
399 2015; 13: 162. <https://doi.org/10.1186/s12967-015-0523-z>
- 400 [23] RUI T, ZHANG X, FENG S, HUANG H, ZHAN S et al. MiR-516a-3p is a Novel Mediator  
401 of Hepatocellular Carcinoma Oncogenic Activity and Cellular Metabolism. *Engineering*  
402 2022; 16: 162-175. <https://doi.org/10.1016/j.eng.2021.07.020>
- 403 [24] MCGEARY SE, LIN KS, SHI CY, PHAM TM, BISARIA N et al. The biochemical basis of  
404 microRNA targeting efficacy. *Science* 2019; 366: eaav1741.  
405 <https://doi.org/10.1126/science.aav1741>
- 406 [25] AGARWAL V, BELL GW, NAM JW, BARTEL DP. Predicting effective microRNA target  
407 sites in mammalian mRNAs. *Elife* 2015; 4: e05005. <https://doi.org/10.7554/eLife.05005>
- 408 [26] LIN S, GREGORY RI. MicroRNA biogenesis pathways in cancer. *Nat Rev Cancer* 2015;  
409 15: 321-333. <https://doi.org/10.1038/nrc3932>
- 410 [27] MOHAMMED J, SIEPEL A, LAI EC. Diverse modes of evolutionary emergence and flux  
411 of conserved microRNA clusters. *RNA* 2014; 20: 1850-1863.  
412 <https://doi.org/10.1261/rna.046805.114>
- 413 [28] WANG Y, LUO J, ZHANG H, LU J. microRNAs in the Same Clusters Evolve to  
414 Coordinately Regulate Functionally Related Genes. *Mol Biol Evol* 2016; 33: 2232-2247.  
415 <https://doi.org/10.1093/molbev/msw089>
- 416 [29] LIN SC, WU HL, YEH LY, YANG CC, KAO SY et al. Activation of the miR-371/372/373  
417 miRNA Cluster Enhances Oncogenicity and Drug Resistance in Oral Carcinoma Cells. *Int J*  
418 *Mol Sci* 2020; 21: 9442. <https://doi.org/10.3390/ijms21249442>
- 419 [30] WENG J, ZHANG H, WANG C, LIANG J, CHEN G et al. miR-373-3p Targets DKK1 to  
420 Promote EMT-Induced Metastasis via the Wnt/ $\beta$ -Catenin Pathway in Tongue Squamous Cell  
421 Carcinoma. *Biomed Res Int* 2017; 2017: 6010926. <https://doi.org/10.1155/2017/6010926>
- 422 [31] HUANG Q, GUMIREDDY K, SCHRIER M, LE SAGE C, NAGEL R et al. The  
423 microRNAs miR-373 and miR-520c promote tumour invasion and metastasis. *Nat Cell Biol*  
424 2008; 10: 202-210. <https://doi.org/10.1038/ncb1681>
- 425 [32] TANG DE, DAI Y, XU Y, LIN LW, LIU DZ et al. The ubiquitinase ZFP91 promotes tumor  
426 cell survival and confers chemoresistance through FOXA1 destabilization. *Carcinogenesis*  
427 2020; 41: 56-66. <https://doi.org/10.1093/carcin/bgz085>
- 428 [33] JIN X, JIN HR, JUNG HS, LEE SJ, LEE JH et al. An atypical E3 ligase zinc finger protein  
429 91 stabilizes and activates NF-kappaB-inducing kinase via Lys63-linked ubiquitination. *J*  
430 *Biol Chem* 2010; 285: 30539-30547. <https://doi.org/10.1074/jbc.M110.129551>
- 431 [34] CHEN D, WANG Y, LU R, JIANG X, CHEN X et al. E3 ligase ZFP91 inhibits  
432 Hepatocellular Carcinoma Metabolism Reprogramming by regulating PKM splicing.  
433 *Theranostics* 2020; 10: 8558-8572. <https://doi.org/10.7150/thno.44873>

- 434 [35] UNOKI M, OKUTSU J, NAKAMURA Y. Identification of a novel human gene, ZFP91,  
435 involved in acute myelogenous leukemia. *Int J Oncol* 2003; 22: 1217-1223.
- 436 [36] PASCHKE L, JOPEK K, SZYSZKAM, TYCZEWSKA M, ZIOLKOWSKA A et al. ZFP91:  
437 A Noncanonical NF- $\kappa$ B Signaling Pathway Regulator with Oncogenic Properties Is  
438 Overexpressed in Prostate Cancer. *Biomed Res Int* 2016; 2016: 6963582.  
439 <https://doi.org/10.1155/2016/6963582>
- 440 [37] MA J, MI C, WANG KS, LEE JJ, JIN X. Zinc finger protein 91 (ZFP91) activates HIF-1 $\alpha$   
441 via NF- $\kappa$ B/p65 to promote proliferation and tumorigenesis of colon cancer. *Oncotarget*.  
442 2016. 7(24): 36551-36562. *Oncotarget* 2016; 7: 36551-36562.  
443 <https://doi.org/10.18632/oncotarget.9070>
- 444 [38] LIU TT, YANG H, ZHUO FF, YANG Z, ZHAO MM et al. Atypical E3 ligase ZFP91  
445 promotes small-molecule-induced E2F2 transcription factor degradation for cancer therapy.  
446 *EBioMedicine* 2022; 86: 104353. <https://doi.org/10.1016/j.ebiom.2022.104353>
- 447 [39] PAN T, YU Z, JIN Z, WU X, WU A et al. Tumor suppressor lnc-CTSLP4 inhibits EMT and  
448 metastasis of gastric cancer by attenuating HNRNPAB-dependent Snail transcription. *Mol*  
449 *Ther Nucleic Acids*. 2021. 23: 1288-1303. *Mol Ther Nucleic Acids* 2021; 23: 1288-1303.  
450 <https://doi.org/10.1016/j.omtn.2021.02.003>

## 452 Figure Legends

454 **Figure 1.** The miR-371-373 cluster was consistently upregulated in gastric cancer. A) The relative  
455 expression levels of the top 20 miRNAs in gastric cancer (calculated as log<sub>2</sub>-fold change). B)  
456 Comparison of the miR-371-373 cluster between gastric cancer and nontumor samples. C) Heatmap  
457 of the miR-371-373 cluster from 411 gastric cancer samples and 42 nontumor samples. \*\*p < 0.01,  
458 \*\*\*p < 0.001, respectively

460 **Figure 2.** The miR-371-373 cluster was negatively correlated with poor survival in gastric cancer. A)  
461 Kaplan-Meier analysis assessed the overall survival of gastric cancer patients with high or low  
462 expression of mir-373, mir-372, and mir-371a. B, C) The 3-year cumulative survival rate and  
463 median survival time of gastric cancer patients with high or low expression of the miR-371-373  
464 cluster. D) The disease-free survival of gastric cancer patients with high or low expression of the  
465 miR-371-373 cluster. E, F) The 3-year disease-free rate and median disease-free time of gastric  
466 cancer patients with high or low expression of the miR-371-373 cluster.

468 **Figure 3.** mir-373 was an independent risk factor for the recurrence and mortality of gastric cancer.  
469 A, B) Univariate and multivariate Cox proportional hazards models for the risk factors for overall

470 survival in gastric cancer. C, D) Univariate and multivariate Cox proportional hazards models for  
471 the risk factors for gastric cancer recurrence. \* $p < 0.05$ , \*\* $p < 0.01$ , \*\*\* $p < 0.001$ , and \*\*\*\* $p <$   
472  $0.0001$ , respectively

473

474 **Figure 4.** mir-373 promoted the malignancy of gastric cancer *in vitro* and *in vivo*. A, B) CCK-8  
475 assay and RTCA detected the proliferation of AGS cells transfected with mir-373 mimics or  
476 inhibitor. C, D) Transwell assays showed the invasion and migration of AGS cells transfected with  
477 mir-373 mimics or inhibitor (40× magnification). E) The xenograft mice model was established by  
478 using AGS cells stably expressing mir-373 and mir-Ctrl. \* $p < 0.05$ , \*\* $p < 0.01$ , \*\*\* $p < 0.001$ ,  
479 respectively

480

481 **Figure 5.** ZFP91 was the direct target of mir-373 in gastric cancer. A-B: KEGG and GO analyses  
482 showed the function of genes that were correlated with mir-373. C: Schematic diagram for the  
483 screening of target genes. D: The expression of ZFP91 and AKIP1 was detected after AGS and  
484 MGC-803 cells were transfected with mir-373 and its controls by western blotting. E-F: Luciferase  
485 reporter assay showed the relative luciferase activities (firefly/Renilla) of wild-type or mutant-type  
486 ZFP91 3' UTR after being affected by mir-373. G-I: Transwell assays and CCK-8 assays showed  
487 the invasion, migration and proliferation of AGS and MGC-803 cells cotransfected with mir-373 or  
488 its control and ZFP91 or its control. \* $p < 0.05$ , \*\* $p < 0.01$ , \*\*\* $p < 0.001$ , \*\*\*\* $p < 0.0001$ ,  
489 respectively

Fig. 1 [Download full resolution image](#)

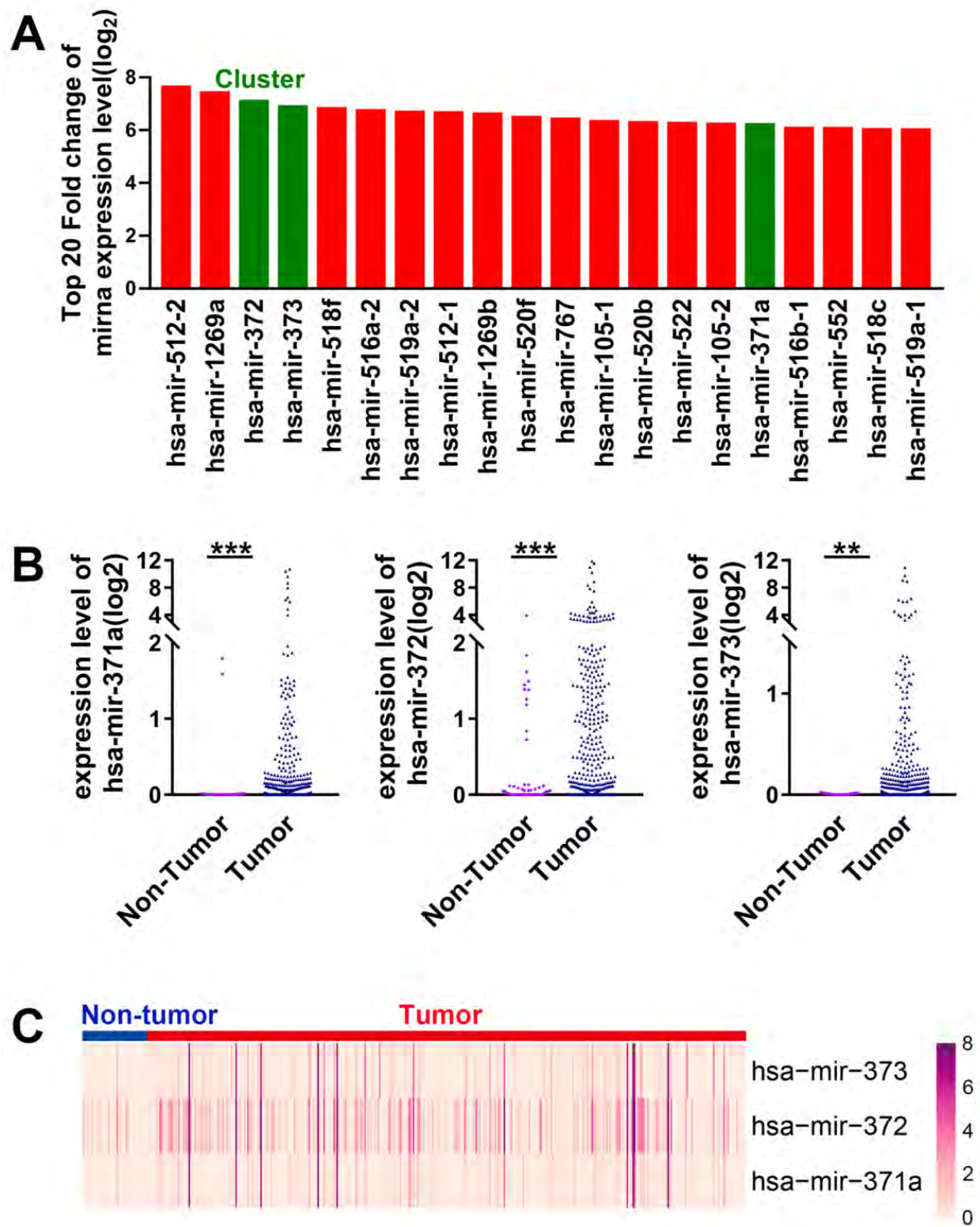




Fig. 2 [Download full resolution image](#)

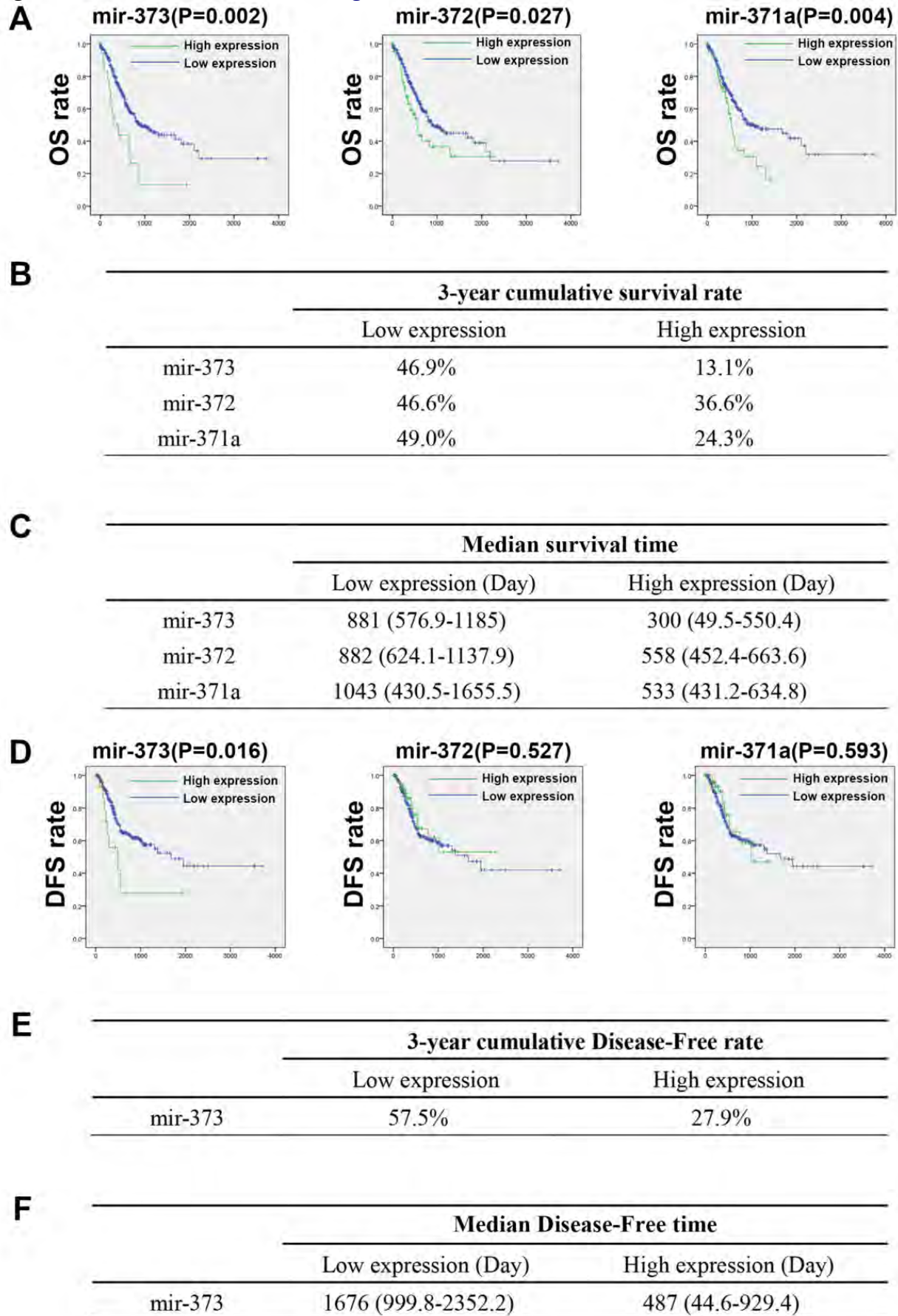


Fig. 3 [Download full resolution image](#)

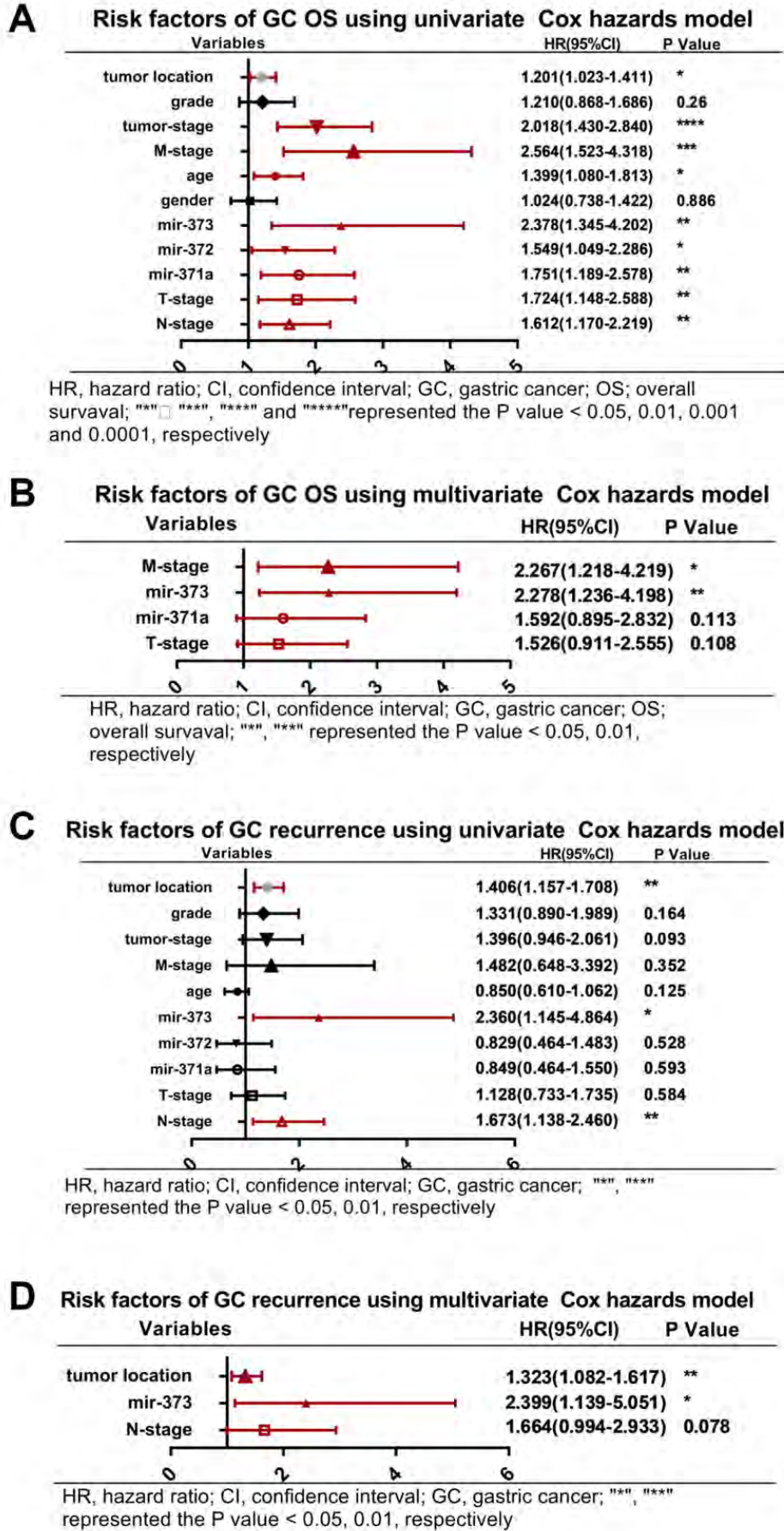




Fig. 4 [Download full resolution image](#)

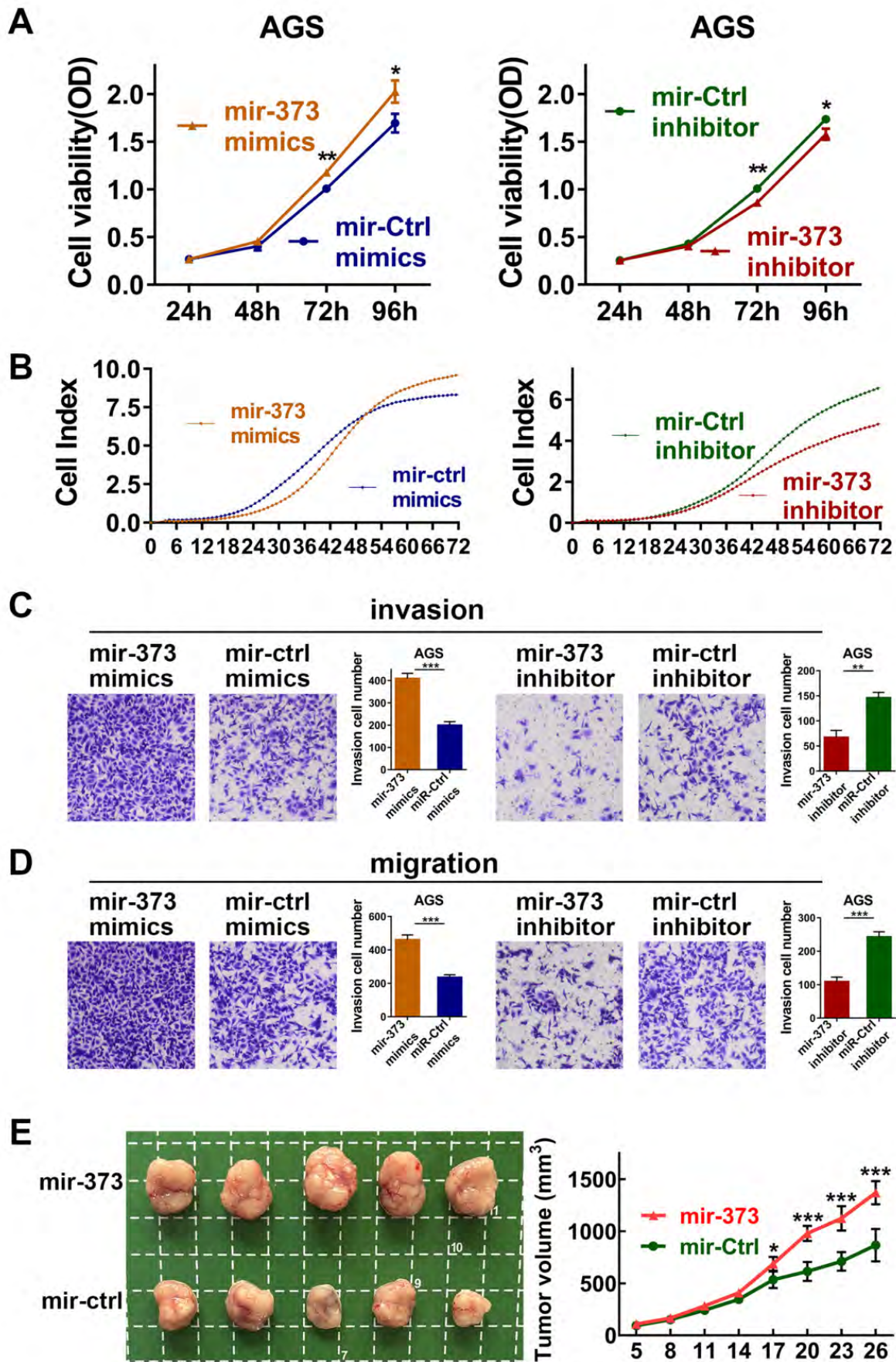


Fig. 5 [Download full resolution image](#)

